USE OF PHASE TRANSPARENCY TO RECONSTRUCT THE PHASE STRUCTURE OF A FIELD

V. A. Zubov, T. V. Mironova, and T. T. Sultanov

A method for reconstructing an optical field is developed. It is based on special shaping of the structure of the information on the amplitude and phase pattern of the recording field. The amplitude information is recorded by a standard method, such as photography. The phase information is recorded after visualization on a phase-sensitive material. The field structure is reconstructed by passing a quasimonochromatic space-coherent plane wave through the obtained transparencies. The method was implemented experimentally for phase-modulated fields with the phase information visualized by the Zernike method.

INTRODUCTION

Phase problems involving recording and reconstruction of an optical field, using two amplitude transparencies, have recently attracted noticeable attraction [1]. The existing methods of reconstructing field by using such transparencies is based on the use of iterations whose number usually exceeds ten [1-3]. In the present paper we consider an approach connected with the reconstruction of the optical field and based on special formation of transparencies with the amplitude and phase information contained in the original field. The phase information is recorded on phase-sensitive material. The field structure is reconstructed by a single pass of a quasimonochromatic space-coherent plane wave through the transparencies. We describe here an experimental realization of the variant of a system for phase-modulated fields.

1. PRINCIPLE OF RECORDING THE PHASE INFORMATION

Assume that a spatially coherent field formed by the object in the xy plane is described by the complex amplitude

$$E(x, y) = a(x, y) \cdot \exp[i\varphi(x, y)] . \tag{1.1}$$

The recording is effected in a two-channel system (Fig. 1) [4]. Information on the distribution of the field amplitudes is recorded in one channel. The other channel records information on the phase by converting the field with filters in the initial xy plane to separate the phase information (if necessary) and in the spatial-frequency plane $\omega_\xi \omega_\eta$ to visualize the phase information.

The distribution of the amplitude information on the object field is recorded in standard fashion. The recording material is acted upon by an intensity distribution produced by the field E(x, y) (1.1),

$$I(x, y) = E(x, y) \cdot E^*(x, y) = a^2(x, y) .$$

Recording on photographic or similar material produces a transparency with a transmission factor

$$T'(x, y) = C_a [I(x, y)]^{-\gamma} ,$$

where C_a is a constant determined by the recording regime and by the characteristics of the material, γ is the material contrast coefficient, and the minus sign preceding γ corresponds to a decrease of the transmission T'(x, y) with increase of the recording intensity I(x, y). The processing conditions are chosen such that $\gamma = -1$. This corresponds to obtaining a positive image or to processing with reversal. In this case the amplitude transmission of the resultant transparency

$$t_a(x, y) = [T'(x, y)]^{1/2} = C_a [I(x, y)]^{-1/2} = C_a \cdot a(x, y)$$

Translated from FIAN Preprint No. 227, Lebedev Physics Institute, Moscow, 1988.

0270-2010/91/1201-0094$12.50

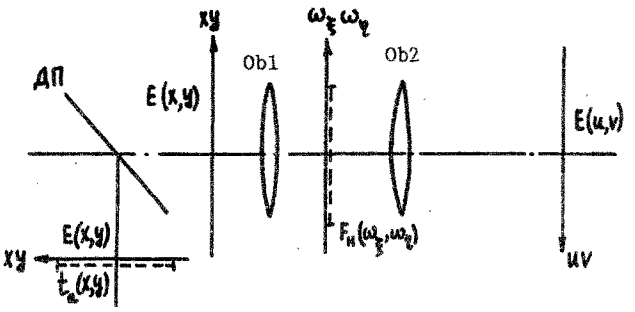

Fig. 1. System for recording field-structure amplitude and phase information on two transparencies.

is determined by the amplitude distribution of the initial optical field, and C_a is a real constant. It must be borne in mind here and henceforth that the field intensities and amplitudes are real positive quantities.

For diffuse or pure phase objects it usually unnecessary to take special measures to separate the phase information. The reason is that at a certain distance from the object the field is characterized by small variations of the amplitude, forming an almost uniform background [5], i.e., the field is described by the expression

$$E'(x,y) = C.\exp[i\varphi(x,y)] ,$$

where C is a real constant

The process of equalizing the amplitude is not analyzed in this case, for in the present study the experiments were performed for fields with phase structure.

To visualize the phase information, the signal is processed in the spatial-frequencies plane $\omega_\xi\omega_\eta$. To this end a Fourier transformation is produced by the system Ob1 with focal length f_1 (see Fig. 1). This yields

$$E(\omega_\xi,\omega_\eta) = -(i/\lambda f_1)\cdot\exp[i(\omega/c)2f_1]\int E'(x,y).\exp[-i(\omega_\xi x+\omega_\eta y)]\,dx\,dy , \qquad (1.2)$$

where $\omega_\xi = \omega\xi/cf_1$, $\omega_\eta = \omega\eta/cf_1$ are the spatial frequencies, and the integral is the Fourier transform of the field E'(x, y). We describe the filtering function by the expression

$$H(x,y) = h(x,y).\exp[i\chi(x,y)] ,$$

which corresponds in the spatial-frequencies plane to a filter of the form

$$F_H(\omega_\xi,\omega_\eta) = \int H(x,y).\exp[-i(\omega_\xi x+\omega_\eta y)]\,dx\,dy .$$

The inverse Fourier transformation is carried out by the optical system Ob2 with focal length f_2 (see Fig. 1), which yields

$$E(\omega_u,\omega_v) = -(i/\lambda f_2)\cdot\exp[i(\omega/c)2f_2]\int E(\omega_\xi,\omega_\eta)\cdot F_H(\omega_\xi,\omega_\eta)\cdot\exp[-i(\omega_u\xi+\omega_v\eta)]\,d\xi\,d\eta \qquad (1.3)$$

where $\omega_u = \omega\cdot u/cf_2$, $\omega_v = \omega\cdot v/cf_2$. The calculations yield ultimately

$$E(u,v) = -(f_1/f_2)\cdot\exp[i(\omega/c)\cdot(2f_1+2f_2)]$$
$$1/4\pi^2\cdot\iint\left[\iint E'(x,y).\exp[-i(\omega_\xi x+\omega_\eta y)]\,dx\,dy\right]\cdot$$
$$\cdot F_H(\omega_\xi,\omega_\eta)\cdot\exp[-i(f_1/f_2)\cdot(\omega_\xi u+\omega_\eta v)]\,d\omega_\xi\,d\omega_\eta .$$

TABLE 1. Parameter of Stepped Wedge M 590005

Number of step,	1	2	3	4	5
$\log H_{rel}$	2,0000	1,8096	1,5775	1,3766	1,1931
Number of step,	6	7	8	9	
$\log H_{rel}$	1,0294	0,8506	0,6981	2,0000	

We change the order of integration and take into account the expression for the inverse Fourier transform of the filtering function H(x, y). As a result we obtain of the convolution of the initial field and of the filtering function

$$E(u,v) = -(f_1/f_2)\cdot\exp[i(\omega/c)\cdot(2f_1+2f_2)]\int E'(x,y).H(-f_1u/f_2-x,-f_1v/f_2-y)\,dx\,dy\,.$$

To simplify the notation it is advantageous to change the directions of the axes u and v and change the scale of these axes, i.e., replace $-(f_1/f_2)$ by u and $-(f_1/f_2)v$ by v. This yields

$$E(u,v) = -(f_1/f_2)\cdot\exp[i(\omega/c)\cdot(2f_1+2f_2)]\int E'(x,y).H(u-x,v-y)\,dx\,dy\,.$$

Various methods can be used to visualize the phase information: the Zernike method, the derivative method, the Foucault knife method, the phase-knife method (Hilbert transformation), and the defocusing method [6, 7]. We consider next a specific variant of the experimental realization of the system using the Zernike method to visualize the phase distribution.

2. TRANSPARENCIES FORMING THE FIELD TO BE RECORDED, AND MEASUREMENT OF THEIR CHARACTERISTICS

The objects used to form the initial field to be recorded were phase transparencies of VRP photographic film. Besides the usual photochemical processing (with the standard developer for this material and with an acid fixing bath), the film was bleached in the following solution;

potassium bichromate	8 g
potassium borate	5 g
concentrated hydrochloric acid	10 ml
water to make	1 liter

Direct interferometer measurement of the phase characteristics of the employed transparencies is quite difficult because of the small scale of the inhomogeneities of their structure. Direct comparison with the unbleached-transparency optical density which is easily measured with a microphotometer was also nonproductive, since a film exposure corresponding to the normal density range yielded small, practically nonmeasurable phase effects. The phase characteristics were determined by a special measurement of the ratio of the normal-range optical densities for different illumination and exposure times with the magnitude of the phase effects obtained by increasing the illumination by a definite number of time. A stepped optical wedge (its parameters are given in Table 1) was used for the photography. Using the wedge, the film was subjected to different exposures t_{exp} and a definite neutral filter with known transmission T_f was used for each exposure (Table 2).

In addition, the film was exposed under the wedge at the same exposure times without neutral filters. The first set of photographs corresponded mainly to the region of normal densities and was used to plot the characteristic curves D = f(log H_{rel}). For the second set, the optical densities were in the overexposure region and yielded phase effects after bleaching. When plotting the characteristic curves, account was taken of the change of the relative exposure $\Delta\log H_{rel}$ introduced by the filter and by the exposure time, assuming that the reciprocity law holds.

In the plots of the phase shift $\Phi = f(\log H_{rel})$ against the exposure account is taken of the effect of the exposure time on the change $\Delta\log H_{rel}$ of the relative exposure. The photography conditions and the values of the arbitrary exposure changes $\Delta\log H_{rel}$ are given in Table 2. The deviation from the reciprocity is not of fundamental significance in this case, for subsequently the comparison was made for photographs with identical exposure times. Measurement of the phase shifts Φ corresponding to definite exposures were made by two methods. The first employed a Mach–Zehnder interferometer. The method is not highly

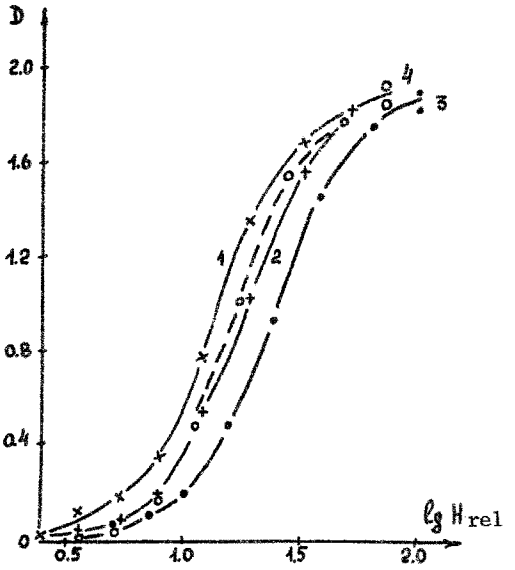

Fig. 2. Characteristic D = f(logH_{rel}) curves for VRP photographic film under different photography conditions: 1) t_{exp} = 10 sec, T_{ph} = 0.5; 2) t_{exp} = 20 sec, T_{ph} = 0.25; 3) t_{exp} = 40 sec, T_{ph} = 0.25; 4) t_{exp} = 80 sec, T_{ph} = 0.09.

sensitive, but ensured measurements of the phase advance that actually occurred when the field was formed by passage of the radiation through the transparency. The second method involved analysis of the pattern of interference between radiation reflected from a glass surface and from the emulsion surface (see Fig. 3). The method was more sensitive but operated in reflected light.

In a Mach–Zehnder interferometer the measured phase shift Φ_{tr} between two sections of a photograph with two surface-relief values l_{em1} and l_{em2} and with different refractive indices n_{em1} and n_{em2} is determined by the expression

$$\Phi_{tr} = (n_{em2}-n_{em1}) \cdot l_{em1} + (n_{em2}-n_a) \cdot l_a ,$$

where $l_a = l_{em2} - l_{em1}$ is the thickness of the air layer, and n_a is the refractive index of the air. For a system with reflection from a photograph, the measured phase shift Φ_{ref} is given by

$$\Phi_{ref} = 2 \cdot (n_{em2} \cdot l_{em2} - n_{em1} \cdot l_{em1}) .$$

The factor 2 describes the double passage of the radiation through the emulsion. A comparison of the methods for the case of the same refractive index $n_{em2} = n_{em1} = n_{em}$ yields

$$\Phi_{ref}/\Phi_{tr} = 2n_{em} \cdot (l_{em2}-l_{em1})/(n_{em}-n_a) \cdot l_a = 2n_{em}/(n_{em}-n_a).$$

(for $n_{em} \sim 1.5$ and $n_a \sim 1.0$ we have $\Phi_{ref}/\Phi_{tr} = 6$).

In the absence of a surface relief, $l_{em2} = l_{em1} = l_{em}$ yields

$$\Phi_{ref}/\Phi_{tr} = 2 \cdot (n_{em2}-n_{em1}) \cdot l_{em}/(n_{em2}-n_{em1}) \cdot l_{em} = 2.$$

One can see a significant increase of the sensitivity in the presence of surface relief. Figure 4 illustrates the measurement of the surface relief by the interferometer method in reflected light.

The dependences of the phase effects Φ_{tr} and Φ_{rel} on the relative exposure log H_{rel}, measured in the Mach–Zehnder scheme and in the reflection scheme, are shown in Figs. 5 and 6. Note that the maximum optical density for the characteristic curves was D_{max} = 1.9 and the maximum phase shift was $\Phi_{tr.max} = 0.26\pi$ and $\Phi_{rel.max} = 0.84\pi$ for the first and second measurement scheme.

The results were used to draw calibration curves (Fig. 7) giving the connection between the phase shift Φ measured in the scheme with reflection and obtained when the exposure was increased, as functions of the optical density D obtained from the characteristic curves. The calibration curves were plotted on the basis of a comparison of the results for identical steps of the

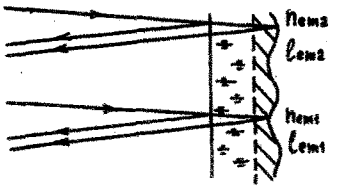

Fig. 3. System for measurement of phase shifts in reflected light.

TABLE 2. Relative Change in Exposure from Photography Conditions

Exposure time (sec)	10	20	40	80
Filter transparency T_f	0,5	0,25	0,25	0,09
Exposure factor:				
for D = $f(\log H_{rel})$	0,5	0,5	1,0	0,72
for Φ = $f(\log H_{rel})$	1,0	2,0	4,0	8,0
$\Delta \lg H_{rel}$				
for D = $f(\log H_{rel})$	-0,301	-0,301	0,0	-0,143
for Φ = $f(\log H_{rel})$	0,0	0,301	0,602	0,903

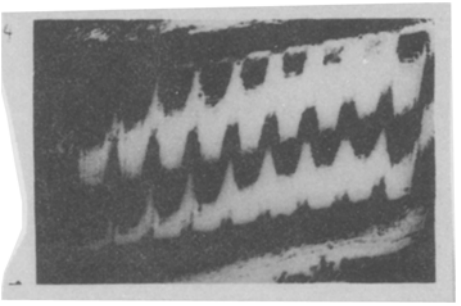

Fig. 4. Illustration of measurement of phase shifts in reflected light.

wedge and identical exposure times. These calibration curves were used to determine the phase characteristics of the transparencies forming the recorded fields, by changing from measurements of the optical density for one photograph to the corresponding phase shift for the other photograph.

We used four types of transparency: random transparency Tr1 with regular structure, formed using a computer random-number program, random transparency Tr2 formed by a speckle structure, transparency Tr3 containing the image of a printed plate. and transparency Tr4 containing a photographic image. The transparencies measured 10 × 10 mm. The transparency exposure conditions are given in Table 3. We measured the optical density D for transparencies obtained by exposure with neutral filters.

The values of D obtained for binary transparencies Tr1 and Tr2 are given in Table 3. For transparencies Tr3 and Tr4 with variable optical density, the table lists the maximum values of the density, D_{max}. Using the corresponding calibration curves (Fig. 7), we determined for each photograph the phase effect produced by it with exposure without the filter Φ_{rel} and Φ_{tr}. These results are also given in the table. For transparencies Tr3 and Tr4 with variable phase effect are given the maximum values of the phase shifts $\Phi_{rel.max}$ and $\Phi_{tr.max}$. Figure 8 shows for illustration prints obtained from transparencies exposed using filters.

3. EXPERIMENTAL REALIZATION OF RECORDING AND RECONSTRUCTION SCHEME

Let us consider the operation of the experimentally realized scheme for formation the needed structure of the output field for recording a phase-modulated field, using a phase transparency (Fig. 9). The initial field distribution is produced at the exit from the transparency Tr_x illuminated by a plane wave with amplitude E, and is described by the complex amplitude [see (1.1)]

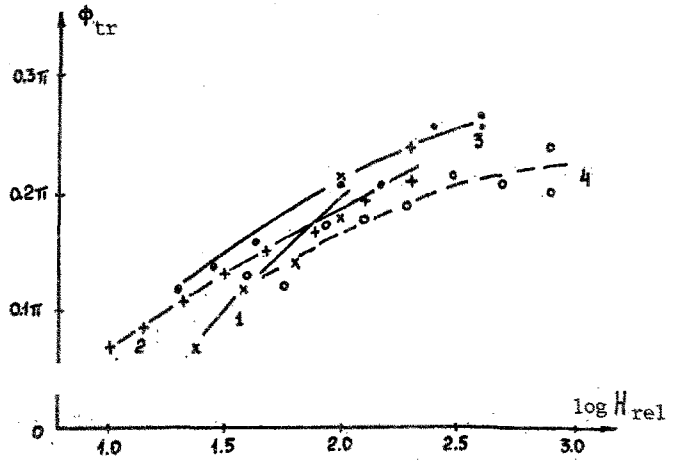

Fig. 5. Dependences of the phase shifts $\Phi_{tr} = f(\log H_{rel})$ on the exposures, measured with a Mach–Zehnder interferometer, under various photography conditions: 1) t_{exp} = 10 sec, 2) t_{exp} = 20 sec, 3) t_{exp} = 40 sec, 4) t_{exp} = 80 sec.

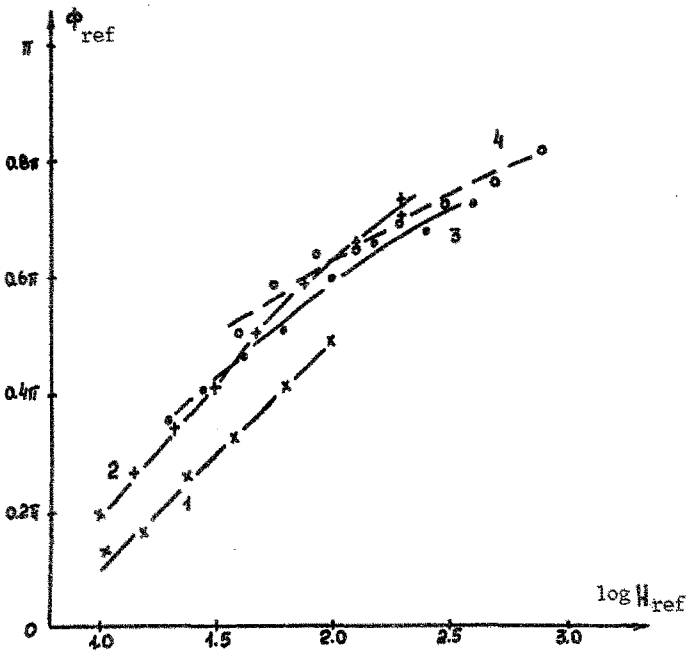

Fig. 6. Dependences of the phase shifts $\Phi_{rel} = f(\log H_{rel})$ on the exposures, measured in reflected light for various photography conditions: 1) t_{exp} = 10 sec, 2) t_{exp} = 20 sec, 3) t_{exp} = 40 sec, 4) t_{exp} = 80 sec..

$$E(x, y) = E_0 \exp[i\varphi(x, y)] .$$

We confine ourselves to a simple variant corresponding to small phase effects $|\varphi(x, y)| << 1$. In this case the quasi-monochromatic spatially coherent field takes the form

$$E(x, y) = E_0 [1 + i\varphi(x, y)] .$$

The reduction that permitted formation of the field structure needed for the recording included in this case a visualization of the phase information. There was no amplitude modulation in the initial field. The reduction was carried out in an optical system effecting a direct and an inverse Fourier transformation. We used in the system reproduction objectives Ob1 and Ob2 of type RF-3 with equal focal lengths $f_1 = f_2 = f = 360$ mm. The transparency Tr_x was located in the forward focal plane

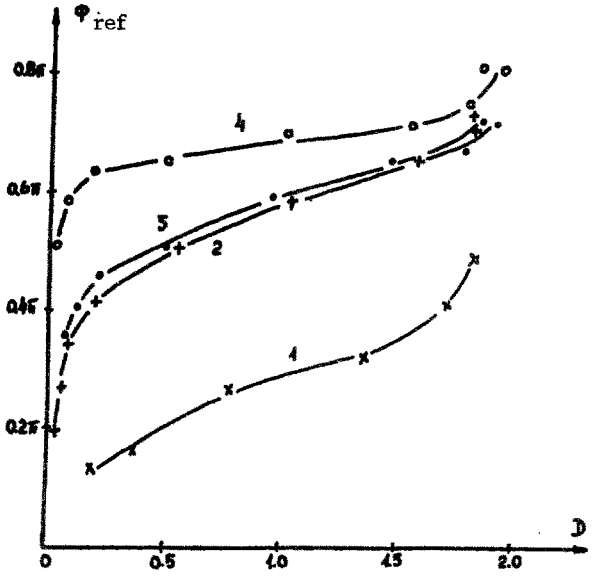

Fig. 7. Calibration curve $\Phi_{rel} = f(D)$ for measurements in reflected light for different exposure times: 1) $t_{exp} = 10$ sec, 2) $t_{exp} = 20$ sec, 3) $t_{exp} = 40$ sec, 4) $t_{exp} = 80$ sec.

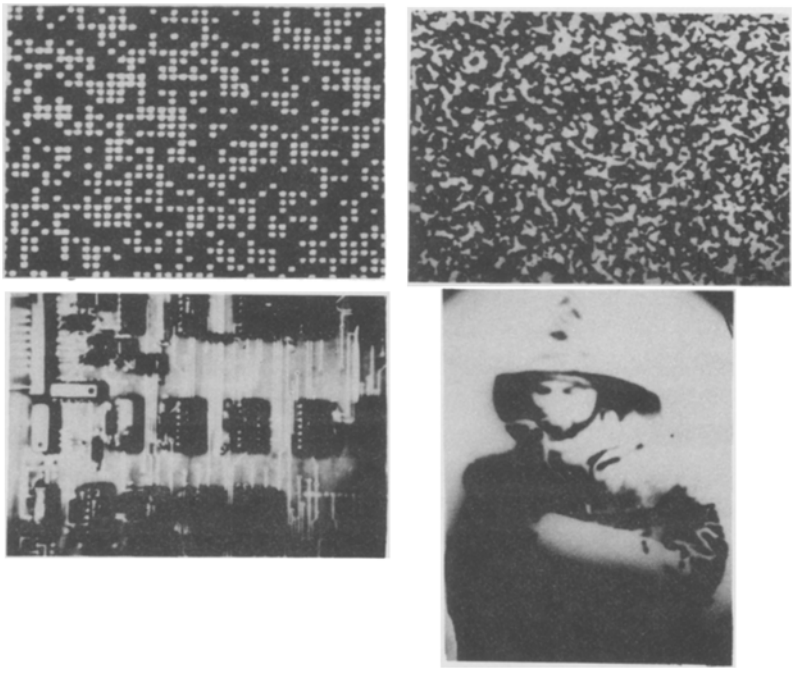

Fig. 8. Illustrative pictures of transparencies used to form the recorded field.

of the first objective Ob1 and was illuminated by a helium–neon laser ($\lambda = 6328$ Å). The optical system Ob1 performed for the field E(x, y) the operation of Fourier transformation [see (1.2)]

$$E(\omega_\xi, \omega_\eta) = -(i/\lambda f)C \cdot \exp[i(\omega/c) \cdot 2f] \cdot [4\pi^2 \cdot \delta(\omega_\xi, \omega_\eta) + iF_\varphi(\omega_\xi, \omega_\eta)],$$

where $F_\varphi(\omega_\xi, \omega_\eta)$ is the Fourier transform of the function $\varphi(x, y)$. In the plane of the spatial frequencies ω_ξ, ω_η we used a Zernike filter visualizing the field and described by a complex amplitude transparency [8]

$$F_H(\omega_\xi, \omega_\eta) = \begin{cases} 1 & \text{for } \omega_\xi, \omega_\eta > \delta\omega_{\xi\eta}, \\ \exp(-i\pi/2)/\tau = -i/\tau & \text{for } \omega_\xi, \omega_\eta < \delta\omega_{\xi\eta}. \end{cases}$$

A filter in a small vicinity $\delta\omega_{\xi\eta}$ of the zero spatial frequencies introduced a $\pi/2$ phase shift and attenuated the amplitude by τ times. For the region of the spatial frequencies ω_ξ, $\omega_\eta > \delta\omega_{\xi\eta}$ the filter performed no transformation whatever. Normal operation of the filter was ensured in the absence from the spectrum of low-frequency spatial object-field frequencies, i.e., in the absence of information on the object field in the range of spatial frequencies $\delta\omega_{\xi\eta}$

TABLE 3. Exposure Conditions for Transparencies Forming the Recorded Field, and Their Characteristics

Transparency	Parameters				
	Exposure time T_s t_{exp} [sec]	Filter transparency T_f	Opt. density D when exposed with filter	Phase effect for exposure without filter φ_{ref}	φ_{tr}
Tr1	10	0,5	1,58	0,12 π	0,31 π
	20	0,25	1,91	0,18 π	0,62 π
	40	0,25	2,00	0,22 π	0,60 π
	80	0,09	2,41	0,21 π	0,70 π
Tr2	10	0,5	2,14	0,22 π	0,51 π
	20	0,25	2,33	0,23 π	0,72 π
	40	0,25	2,58	0,25 π	0,71 π
	80	0,09	2,75	0,22 π	0,78 π
Tr3	20	0,25	1,97	0,19 π	0,60 π
Tr4	20	0,25	2,42	0,23 π	0,67 π

$$F_{\varphi}(\omega_{\xi}, \omega_{\eta}) = 0 \quad \text{or} \quad \omega_{\xi}, \omega_{\eta} < \delta\omega_{\xi\eta} .$$

In the exit plane, which is the rear focal plane of the second objective Ob2, there was formed a field corresponding to the inverse Fourier transform

$$E(\omega_u, \omega_v) = -[1/(\lambda f)^2] \cdot C_e \cdot \exp[i(\omega/c)4f] \cdot \int [4\pi^2 \cdot \delta(\omega_{\xi}, \omega_{\eta}) + iF_{\varphi}(\omega_{\xi}, \omega_{\eta})] \cdot (-i/\tau) \cdot F_H(\omega_{\xi}, \omega_{\eta}) \exp[-i(\omega_u \xi + \omega_v \eta)] \, d\xi \, d\eta .$$

The optical systems Ob1 and Ob2 had identical parameters ($f_1 = f_2 = f$). As a result, the scales of the field structures were the same in the planes xy and uv. The result was formation of a field with visualized phase information in the exit plane:

$$E(u, v) = -iC \cdot [1/\tau - \psi(u, v)] \cdot \exp[i(\omega/c) \cdot 4f] .$$

The information should be recorded on a material having a phase response, such as bleached emulsion, chromium-treated gelatine, photothermoplastic, and others [9]. The scheme realized recorded photographically the obtained information in the form of the intensity distribution

$$I(u, v) = E(u, v) \cdot E^*(u, v) = C^2 \cdot [1/\tau^2 - 2 \cdot \varphi(u, v)/\tau] .$$

(it is assumed here that $1/\tau >> |\varphi(u, v)|$, and terms of second order of smallness are omitted). The recording material was MIKRAT-300, processed in the usual manner (development and fixation in an acid fixing solution). To form the transparent structure $t_{in}(u, v)$ needed to reproduce the initial field, it is necessary to maintain certain photography and processing conditions [4] that ensure a definite magnitude and sign of the phase effect. In our study, a transparent Tr_B that makes it possible to reconstruct the field was formed by reprinting the photograph from the MIKRAT-300 material to the VRP material for which the amplitude and phase characteristics were investigated (Figs. 2, 5, and 6). The reprinting of the photograph was not of fundamental significance, but simplified substantially the choice of the photography and processing conditions in the investigation of the considered variant of the phase-problem solution, and ensured automatically the correct sign of the phase effect. Bleaching produced in such a material a transparency with a complex amplitude transmission

$$t_{in}(u, v) = \exp[-ib \cdot (I(u, v))^{\gamma}] = \exp[-ibC^2 \cdot (1/\tau^2 - 2 \cdot \varphi(u, v)/\tau)^{\gamma}] ,$$

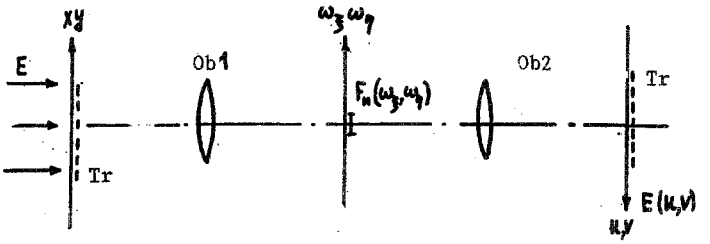

Fig. 9. Scheme for formation of the structure of a recorded phase field using a Zernike filter.

where the constant coefficients b and C and the parameter γ were determined by the regimes for the recording and for the processing of the photographic material. The conditions for recording the phase information (the constant b), the filtering conditions (the constant τ), and the conditions for separating the phase information (the constant C) were chosen such that $\gamma = 1$ and $2bC^2/\tau = 1$. This ensured formation of a transparency whose complex amplitude transmission coincided, accurate to a complex constant, with the phase structure of the field

$$t_{in}(u, v) = C_{in} \cdot \exp[i\varphi(u, v)] .$$

In the experimental realization, the exposure times of the VRP material were chosen as before from the set t_{exp} = 10, 20, 40, 80 sec, and the exposure was carried out both without a filter and with a corresponding filter having a transmission T_f = 0.5, 0.25, 0.25, 0.09 (see Table 2). Photographs exposed without attenuating filters were bleached and used as transparencies Tr_B that made it possible to reproduce, by transmitted light, the structure of the initial field. Satisfaction of the necessary photography conditions was achieved on the basis information provided by a calibration plot $\Phi_{ref} = f(D)$. With the aid of the plot it is possible to determine, from the optical density D_{in} of the photograph taken with a filter, the value of the produced phase effect Φ_{rel} for exposure of the VRP material without a corresponding filter. By choosing exposure conditions such that the optical density D_{in} of the formed transparency coincided with the optical density D of the initial transparency (we have in mind transparencies exposed through filters), we obtained identical phase transparencies Tr_B and Tr_x also for photographs taken without filters but bleached.

The object field was reconstructed by passing through the transparency $t_{in}(u, v)$ a plane light wave of amplitude E_0. Clearly, use of the constructed transparency will lead to formation of a field with complex amplitude

$$E(u, v) = E_0 \cdot t_{in}(u, v) = E_0' \cdot \exp[i\varphi(u, v)] ,$$

duplicating, apart from a complex constant, the initial recorded field formed by the object.

As an additional check that the passage of monochromatic spatially coherent radiation produces through the obtained transparency Tr_B a field that agrees with the one produced by the initial transparency Tr_x, we compared the spatial-frequency spectra for the fields produced by these transparencies. The spatial-frequency spectrum was produced by objective RF-3 with focal length f = 360 mm. The intensity distribution in the spatial-frequency spectrum was recorded by a slotted photomultiplier and a V-7-21 digital voltmeter. The experimental results are shown in Fig. 10 for the random transparencies Tr1 and Tr2. The point spacings were 0.5 and 0.1 mm for transparencies Tr1 and Tr2, respectively. The abscissa is the geometric coordinate corresponding to the spatial frequency ω_ξ in the section passing through the origin (this direction is indicated in Fig. 8). The ordinates are, in logarithmic scale, the relative values of the intensities $I_{\omega\xi}$ for the spatial frequencies. The choice of the scale is governed by the large intensity differences in the zero-frequency and shifted-frequency regions. There was no need for special intensity normalization. The values agreed with good accuracy, since the transparencies had the same transmission due to the bleaching and to the choice of exposure and processing of the photographic material to obtain identical optical densities. The solid curves in the figure correspond to the initial transparency Tr_x, and the points to the transparency Tr_B used to reconstruct the field structure. It can be seen from the plots that the spatial-frequency spectra are in agreement. It should be noted, to be sure, that the figure shows a noticeable disparity of the field structures in the regions corresponding to low intensity in the spatial-frequency spectrum ($I_{\omega\xi}$ < 3-5 in the units shown in the figures, and $I_{\omega\xi} < 0.01 I_{\omega\xi max}$ in relative units). This disparity is due to the speckle structure formed during the stage of visualization of the phase information and formation of the transparency Tr_B. The maximum speckle-structure scale is determined by the ratio $\Delta\xi = \lambda f/D$, where f is the focal length of the objective and D is the light-beam diameter. The corresponding spatial frequency is equal to $\omega_\xi = 2\pi/\Delta\xi$. For a light-beam diameter ~2 mm

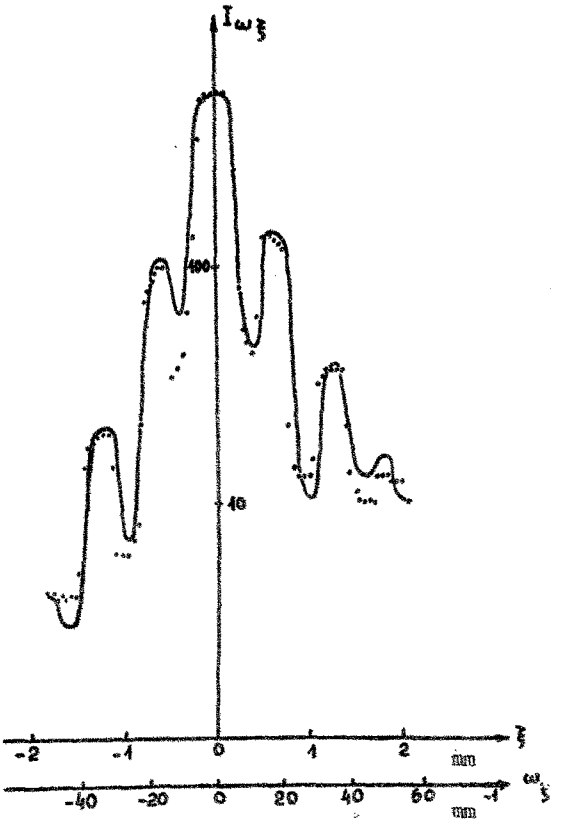

Fig. 10a. Comparison of the spatial-frequency spectra for the initial regular random transparency Tr_x (solid line) and for the formed transparency Tr_B (points).

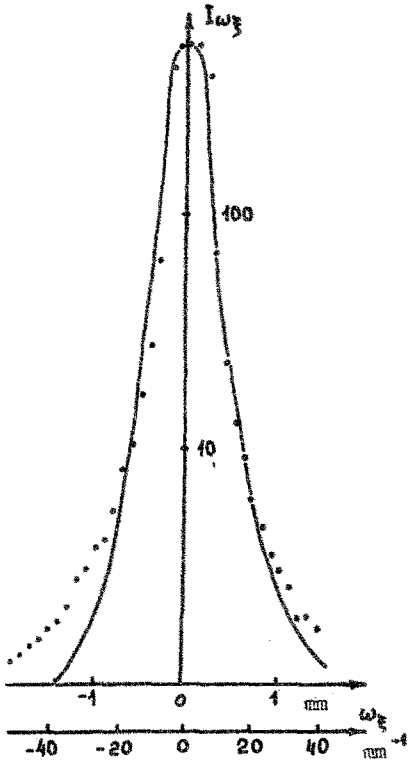

Fig. 10b. Comparison of the spatial-frequency spectra for the initial irregular random transparency Tr_x (solid line) and for the formed transparency Tr_B (points).

TABLE 4. Errors in the Reconstruction of the Spatial-Frequency Spectra

Transparency	n	S^2	S	n	S^2	S
Tr1	78	397	19,9	76	190	13,8
Tr2	29	240	15,5	27	73	8,6

and for an objective with focal length 360 mm we have $\Delta\xi \sim 0.11$ mm and $\omega_\xi \sim 60$ mm^{-1}. The dimension of the periodic-structure elements on the transparency is d ~ 0.4 mm. Thus, the speckle structure can indeed make a noticeable contribution to the spectrum observed on reconstruction of the field.

A quantitative comparison of the spatial-frequency spectra was based on the sampling variance

$$S^2 = (\Sigma\, \Delta I_n^2)/(n-1)$$

or the sampling standard deviation S. In this expression $\Delta I_n = I_{n\,in} - I_{n\,out}$, $I_{n\,in}$, $I_{n\,out}$ are the intensities for a definite point of the spatial frequencies, for fields from the initial transparency Tr_x and from the reconstructed transparency Tr_B. The results for S^2 and S are given in Table 4.

The main contribution to the indicated quantities is made by the points corresponding to sections in which the intensities $I_{\omega\xi}$ change abruptly. If two such points are excluded for each transparency, the values of S^2 and S decrease noticeably. These numbers are also shown in Table 4.

The discard of these points can be based on the excess of the significance levels for the experimentally obtained errors. The average error for the complete set of measurements is equal to −4 and −5.8 for random regular and irregular transparencies. The significance level is defined as [10]

$$\overline{\Delta I}_{\omega\xi} + g_{en} \cdot S$$

The coefficient g_{en} is equal to ~3 for the significance level ~0.05 and for 78 and 29 measurements. This yields significance levels ~60 and ~45 respectively for regular and irregular random transparencies. Larger values of $\Delta I_{\omega\xi}$ can therefore be attributed to large measurement errors and excluded from consideration.

Let us estimate the effect of the errors on the results of the considered scheme. For a transparency obtained by copying on VRP material and bleaching, the amplitude transparency is described by the expression

$$t_{in}(u, v) = \exp[-ib \cdot (I(u, v))^{\gamma}] .$$

We use for the calculation a dimensionless intensity representation $I(u, v)/I_m$ for the case of registration of the transparency Tr_B intended to reconstruct the field, where I_m is the maximum value in the intensity distribution. For registration of a transparency under real conditions different from the required ones we have

$$t_{in}(u, v) = \exp[-i(b \pm \Delta b) \cdot (I(u, v))^{\gamma \pm \Delta\gamma}] .$$

A series expansion yields

$$[I(u, v)]^{\gamma \pm \Delta\gamma} = [I(u, v)]^{\gamma} \cdot [1 \pm \Delta\gamma \cdot \ln(I(u, v)/I_m)] = [I(u, v)]^{\gamma} \cdot [1 \pm \Delta\gamma \cdot \ln(I_m/I(u, v))] .$$

The relative error $\Delta\varphi_1/\varphi(u, v)$ due to deviation of the real reduction conditions from the needed ones ($\gamma \pm \Delta\gamma$) is thus

$$\Delta\varphi_1/\varphi(u, v) = \Delta\gamma \cdot \ln[I_m/I(u, v)] .$$

The relative error $\Delta\varphi_2/\varphi(u, v)$ due to deviation of the real conditions for the formation of the transparency $t_{out}(u, v)$ from the needed ones ($b \pm \Delta b$) is described by an error of b

$$\varphi(u, v) \pm \Delta\varphi_2 \sim b \pm \Delta b = b \cdot (1 \pm \Delta b/b)$$

and

$$\Delta\varphi_2/\varphi(u, v) = \Delta b/b .$$

In addition, the physical transparency $t_{out}(u, v)$ contains errors $\Delta\varphi_3/\varphi(u, v)$ due to the random errors of the recording process itself. As a result we obtain for the total error

$$[\Delta\varphi/\varphi(u,v)]^2 = [\Delta\gamma \cdot \ln(I_m/I(u,v))]^2 + [\Delta\varphi_2/\varphi(u,v)]^2 + [\Delta\varphi_3/\varphi(u,v)]^2 .$$

We present now numerical estimates for the following values: intensity-variation range ~100

$$I_m/I(u,v) \sim 100 ,$$

relative error of contrast coefficient ~1%

$$\Delta\gamma \sim 0,01 \text{ for } \gamma = 1 ,$$

relative error in the conditions of the phase transparency reduction ~2%

$$\Delta b/b \sim 0,02 ,$$

Relative error connected with the registration process itself — random registration error (graininess) ~2%

$$\varphi_3/\varphi(u,v) \sim 0,02 .$$

The numerical calculation yields ultimately

$$\Delta\varphi/\varphi(u,v) \sim 0,05 .$$

The above results and error estimates show that when certain requirements are met by the object field structure (no low frequencies in the spatial-frequency spectrum, small phase actions), using a quasimonochromatic spatially coherent radiation, and using the phase method of recording the phase information it is possible in principle to record information on the light field, followed by its reconstruction, for a specially formed structure of the recorded field and of the recorded phase information, in the form of a transparency with a phase response. The effect in the recorded field can reach $\pi/4$. The field structure is recorded by illuminating the obtained transparency with a plane quasimonochromatic spatially coherent wave.

Further progress in the direction considered is assumed to follow the line of decreasing the limitations connected with visualization of the phase information, and of changing to gas-discharge light sources to decrease the influence of the speckle structure of the light filed formed in the intermediate state.

The authors thank G. G. Petrash for interest in the work and I. I. Sobel'man for helpful discussions.

LITERATURE CITED

1. Kh. A. Ferverda, "The problem of reconstructing the phase of a wave front from the amplitude distributions and the error functions," in: Inverse Problems in Optics [in Russian], Mashinostroenie, Moscow (1984), pp. 21-47.
2. P. Kiedron, "Conditions sufficient for a one-dimensional unique recovery of the phase under assumption that the image intensity distributions: $f(x)^2$ and $(d^2f/dx^2)^2$ are known," Optica Applicata, **10**, No. 2, 149-154 (1980).
3. T. I. Kuznetsova and D. Yu. Kuznetsov, "Reconstruction of phase characteristics with the aid of active optical systems," Kvantovaya Élektron. (Moscow), **12**, No. 12, 2507-2509 (1985).
4. V. A. Zubov, "Reconstruction of the characteristics of an optical field using amplitude and phase transparencies," Kvantovaya Élektron. (Moscow), **14**, No. 8, 1215-1217 (1987).
5. A. A. Akaev and S. A. Maiorov, Coherent Optical Computers [in Russian], Mashinostroenie, Leningrad (1977), Part II, Chap. 8, Sec. 8.1., pp. 310-320.
6. J. B. de Velis and G. G. Reynolds, Theory and Application of Holography, Addison-Wesley (1967) Chap. 8.
7. A. M. Soroko, Hilbert-Optics [in Russian], Nauka, Moscow (1981). Chap. 2, Secs. 2.2 and 2.3, Chap. 3, Sec. 3.1.
8. M. Born and E. Wolf, Principles of Optics, Pergamon (1970), Chap. 8. Sec. 8.6.3.
9. V. A. Varshavskii (ed.), in: Silver-Free and Unusual Holography Media [in Russian], Nauka, Leningrad (1983), pp. 10-24, 51-80.
   V. A. Varshavskii (ed.), in: New Recording Media for Holography [in Russian], Nauka, Leningrad (1983), pp. 16-22, 101-106, 122-130.
   L. A. Kortuzhanskii (ed.), in: Silver-Free Photographic Materials [in Russian], Khimiya, Leningrad (1984).

10. V. N. Lavrenchik, Organization of Physical Experiment and Statistical Reduction of Its Results [in Russian], Moscow, Énergoatomizdat (1966), Chap. 5, Sec. 5.13, pp. 176-178.